# The structure and cooling of massive compact stars

Armen Sedrakian

in collaboration with
L. Bonanno, G. Colucci, D. Hess, X.-G. Huang, D. Rischke, M. Sinha

Institute for Theoretical Physics,
J. W. Goethe University, Frankfurt Main, Germany

EMMI Workshop “Dense baryonic matter in the cosmos and the laboratory”

# Outline

- Recent experimental motivation

- Description of dense bulk nuclear matter at and above the saturation density
- Ground state properties vs neutron star observations (Demorest pulsar)

- Superfluidity, excitations, and response functions
- CAS A: a cooling quark star?

# A two-solar-mass neutron star measured

## The largest pulsating star yet observed casts doubts on exotic matter theories

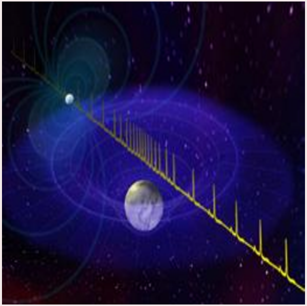

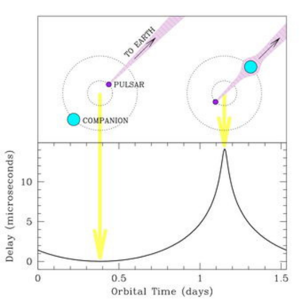


The binary millisecond pulsar J1614-223010+11 Shapiro delay signature:

$$\Delta t = -\frac{2GM}{c^3}\log(1 - \vec{R}\cdot\vec{R}'). \qquad (1)$$

The pulsars mass $1.97 \pm 0.04$ solar masses which rules out almost all currently proposed hyperon or boson condensate equations of state. (Demorest et al, 2010, Nature 467, 1081)

# Cas A remnant, cooling in course

This extraordinarily deep Chandra image shows Cassiopeia A (Cas A, for short), the youngest supernova remnant in the Milky Way.

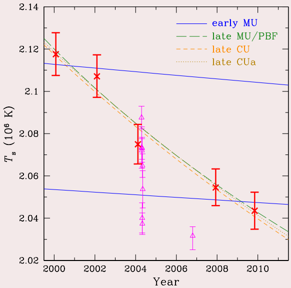


NASA's Chandra X-ray Observatory has discovered the first direct evidence for a superfluid. (Conclusions drawn from cooling simulations of the neutron stars).

# I. Dense Matter Equation of State and Neutron Stars

# Relativistic covariant Lagrangians for hadronic and quark phases

**Boguta-Bodmer-Walecka Lagrangian for effective fields:**

$$
\begin{aligned}
\mathcal{L}_B \quad = \quad & \sum_B \bar{\psi}_B[\gamma^\mu(i\partial_\mu - g_{\omega B}\omega_\mu - \frac{1}{2}g_{\rho B}\boldsymbol{\tau}\cdot\boldsymbol{\rho}_\mu) - (m_B - g_{\sigma B}\sigma)]\psi_B + \frac{1}{2}\partial^\mu\sigma\partial_\mu\sigma \\
& -\frac{1}{2}m_\sigma^2\sigma^2 + \frac{1}{2}m_\omega^2\omega^\mu\omega_\mu - \frac{1}{4}\boldsymbol{\rho}^{\mu\nu}\cdot\boldsymbol{\rho}_{\mu\nu} + \frac{1}{2}m_\rho^2\boldsymbol{\rho}^\mu\cdot\boldsymbol{\rho}_\mu \\
& -\frac{1}{3}bm_N(g_{\sigma N}\sigma)^3 - \frac{1}{4}c(g_{\sigma N}\sigma)^4 + \sum_{e^-,\mu^-}\bar{\psi}_\lambda(i\gamma^\mu\partial_\mu - m_\lambda)\psi_\lambda - \frac{1}{4}F^{\mu\nu}F_{\mu\nu},
\end{aligned}
$$

- The model is viewed as a Density Functional Theory
- $B$-sum is over the baryonic octet $B \equiv p, n, \Lambda, \Sigma^{\pm,0}, \Xi^{-,0}$
- $N$-meson sector $g_{\sigma N}/m_\sigma = 3.967$ $g_{\omega N}/m_\omega = 3.244$ $g_{\rho N}/m_\rho = 1.157$ fm
- $H$-meson couplings weaker by factors 0.6, 0.658, 0.6.
- GM3 parametrization, Glendenning & Moszkowski 1991, PRL, 67, 2414

# Quark phases

**Nambu-Jona-Lasinio Lagrangian:**

$$\begin{aligned}\mathcal{L}_Q &= \bar{\psi}(i\gamma^\mu\partial_\mu - \hat{m})\psi + G_V(\bar{\psi}i\gamma^0\psi)^2 + G_S\sum_{a=0}^{8}[(\bar{\psi}\lambda_a\psi)^2 + (\bar{\psi}i\gamma_5\lambda_a\psi)^2] \\ &+ G_D\sum_{\gamma,c}[\bar{\psi}^a_\alpha i\gamma_5\epsilon^{\alpha\beta\gamma}\epsilon_{abc}(\psi_C)^b_\beta][(\bar{\psi}_C)^r_\rho i\gamma_5\epsilon^{\rho\sigma\gamma}\epsilon_{rsc}\psi^8_\sigma] \\ &- K\left\{\det{}_f[\bar{\psi}(1+\gamma_5)\psi] + \det{}_f[\bar{\psi}(1-\gamma_5)\psi]\right\}, \qquad (2)\end{aligned}$$

quark spinor fields $\psi^a_\alpha$, color $a = r, g, b$, flavor ($\alpha = u, d, s$) indices, mass matrix $\hat{m} = \mathrm{diag}_f(m_u, m_d, m_s)$, $\lambda_a$ $a = 1, \dots, 8$ Gell-Mann matrices. Charge conjugated $\psi_C = C\bar{\psi}^T$ and $\bar{\psi}_C = \psi^T C$ $C = i\gamma^2\gamma^0$.

- $a$ sum is over the 8 gluons
- $G_S$ is the scalar coupling fixed from vacuum physics; $G_D$ is the scalar coupling, which is related to the $G_S$ via Fierz transformation
- $G_D$ is treated as a free parameter

# Quark phases

Pairing patterns: Order parameter

$$\Delta \propto \langle 0|\psi^a_{\alpha\sigma}\psi^b_{\beta\tau}|0\rangle$$

- Antisymmetry in spin $\sigma, \tau$ for the BCS mechanism to work
- Antisymmetry in color $a, b$ for attraction
- Antisymmetry in flavor to avoid Pauli blocking

At low densities 2SC phase (Bailin and Love '84)

$$\Delta \propto = \Delta_0 \epsilon^{ab3} \epsilon_{\alpha\beta}$$

But most likely with broken spatial symmetries due to beta-equilibrium ! (see later)

At high densities we expect 3 flavors of $u, d, s$ massless quarks. The ground state is the color-flavor-locked phase (Alford, Rajagopal, Wilczek '99)

$$\Delta \propto \langle 0|\psi^a_{\alpha L}\psi^b_{\beta L}|0\rangle = -\langle 0|\psi^a_{\alpha R}\psi^b_{\beta R}|0\rangle = \Delta\epsilon^{abC}\Delta\epsilon_{\alpha\beta C}$$

The partition function is evaluated in the mean field approximation.

# EoS with equilibrium among nuclear, hyperonic, 2SC- and CFL-quark phases

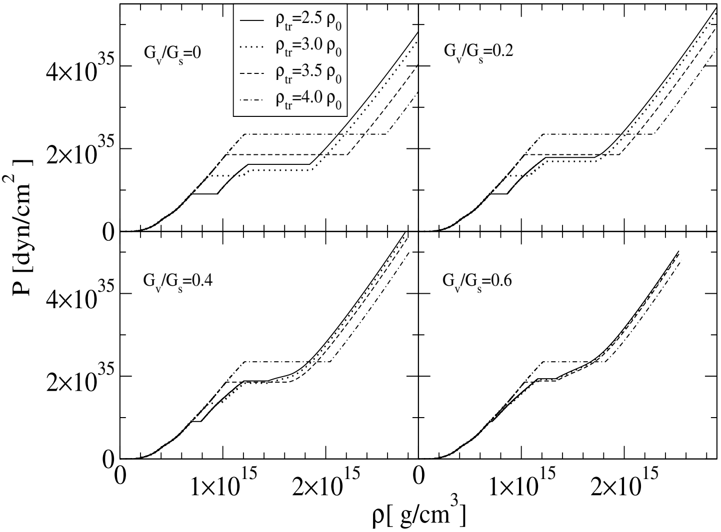

# Mass vs Radius relationship

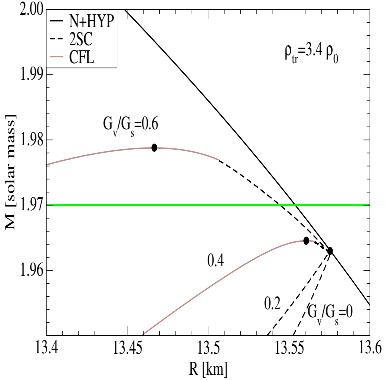


- Dashed only 2SC, grey includes CFL.
- Stability is achieved for $G_V > 0.2$ and transition densities few $\rho_0$
- Left panel: Rapidly rotating stars may not have counterparts in the static limit

# Composition: multilayer stars with quark, hyperonic, nuclear matters

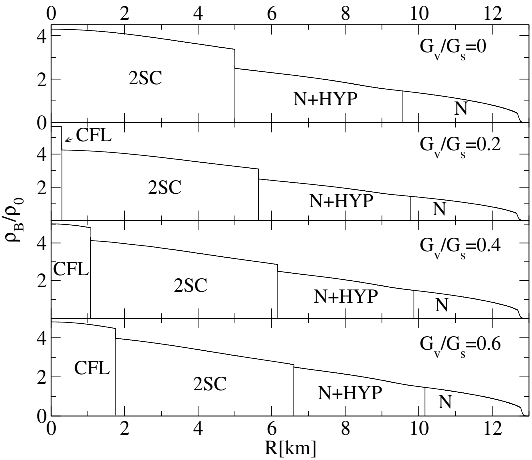


- Fix transition density $2.5 \times \rho_0$.
- Increasing $G_V$ stabilizes the stars + "exotic matter"

# Equation of state conclusions

- To produce heavy and exotics featuring neutron stars it is sufficient a stiff NM equation state above saturation.
- Furthermore, we need vector interactions to stabilize color superconducting quark star.
- A $2M_{\odot}$ mass star does not exclude exotic matter in the cores of NS
- Others possibilities modifications in the hyperonic sector (repulsive vector interactions)
- Modification of the gravity is also a possibility

- improvements in the range $0.5 \leq \rho/\rho_0 \leq 2$ should be possible with the use of microscopically motivated models
- Quark matter EoS can be constrained at high densities by perturbative QCD results

more detailes: L. Bonanno, A. Sedrakian, Astron. and Astrophys. vol. 539, A16 (2012).

# II. Cooling of neutron stars

# Cooling of compact stars

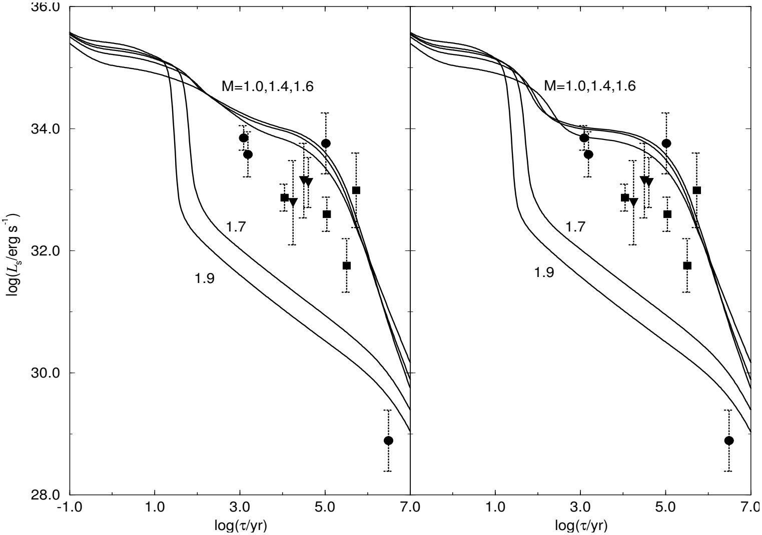

Energy balance equation (Thorne '77)

$$\frac{d}{dr}\left(Le^{2\Phi}\right) = \frac{-4\pi r^2}{\sqrt{1-\frac{2Gm}{rc^2}}} ne^{\Phi} T \frac{ds}{dt}. \tag{3}$$

$L$ is the total luminosity (neutrino + photon) The gradients of neutrino luminosity

$$\frac{d}{dr}\left(L_\nu e^{2\Phi}\right) = \frac{4\pi r^2}{\sqrt{1-\frac{2Gm}{rc^2}}} ne^{2\Phi} q_\nu, \qquad \frac{d}{dr}\left(Te^{\Phi}\right) = \frac{-3\kappa\rho}{16\sigma T^3} \frac{L_\gamma e^{\Phi}}{4\pi r^2\sqrt{1-\frac{2Gm}{rc^2}}} \tag{4}$$

In isothermal core approximation $T' = Te^{\Phi} = \text{const.}$

$$\boxed{\frac{dT'}{dt} = -\frac{\int_0^{R_c} nq_\nu(r,T)e^{2\Phi}dV_p + 4\pi\sigma R^2 T_S^4 e^{2\Phi_c}}{\int_0^{R_c} nc_v(r,T)dV_p}.} \tag{5}$$

## Key processes

- Modified Urca process

$$n + n \to n + p + e + \bar{\nu},$$

- Crust bremsstrahlung

$$e + (A, Z) \to e + (A, Z) + \nu + \bar{\nu},$$

- Pair-breaking processes

$$[NN] \to [NN] + \nu + \bar{\nu}.$$

- Photo-emission from the surface

$$L_\gamma = 4\pi\sigma R^2 T^4$$

III. Non-standard (exotic) cooling of neutron stars

# Cooling processes in quark matter

Quark cores of NS emit neutrons via: $d \to u + e + \bar{\nu}_e \quad u + e \to d + \nu_e$. The rate of the process is The neutrino emissivity is expressed in terms of the polarization tensor of baryonic matter

$$\varepsilon_{\nu\bar{\nu}} = -2\left(\frac{G_F}{2\sqrt{2}}\right)^2 \int d^4q g(\omega)\omega \sum_{i=1,2}\int \frac{d^3q_i}{(2\pi)^3 2\omega_i}\Im[L^{\mu\lambda}(q_i)\,\Pi_{\mu\lambda}(q)]\delta^{(4)}(q-\sum_i q_i),$$

The response function *at one loop*

$$\Pi_{\mu\lambda}(q) = -i\int\frac{d^4p}{(2\pi)^4}\mathrm{Tr}\left[(\Gamma_-)_\mu S(p)(\Gamma_+)_\lambda S(p+q)\right], \quad \Gamma_\pm(q) = \gamma_\mu(1-\gamma_5)\otimes\tau_\pm$$

with propagators

$$S_{f=u,d} = i\delta_{ab}\frac{\Lambda^+(p)}{p_0^2-\epsilon_p^2}(\not{p}-\mu_f\gamma_0), \quad F(p) = -i\epsilon_{ab3}\epsilon_{fg}\Delta\frac{\Lambda^+(p)}{p_0^2-\epsilon_p^2}\gamma_5 C$$

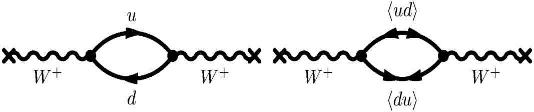


(a) (b)

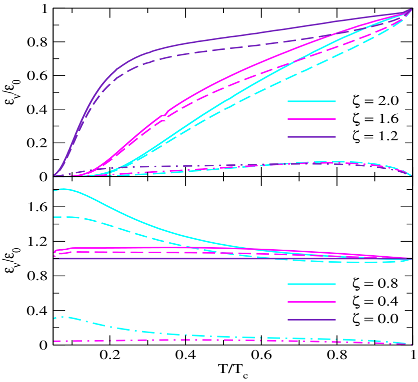


Gapless vs gapped emissivities (P. Jaikumar, C. Roberts, A. Sedrakian, Phys. Rev. C73: 042801, 2006)
Here $\zeta = \Delta/\delta\mu$, where $\delta\mu = \mu_d - \mu_u = \mu_e$.

One loop calculations may not be enough!

The vector conservation in baryonic matter is recovered only when full re-summation of polarization tensors is carried out!

In the case of one loop EFT in powers of $v_F/c$ (Leinson-Perez '06, Sedrakian-Müther-Schuck '07, Kolomeitsev-Voskresensky '08)

$$\epsilon_V \propto O(1), \qquad \epsilon_V \propto v_F^4.$$

To describe a superfluid we need the propagators

$$\mathcal{G}_{\sigma,\sigma'}(i\omega_n,\boldsymbol{p}) = \begin{pmatrix} \hat{G}_{\sigma\sigma'}(i\omega_n,\boldsymbol{p}) & \hat{F}_{\sigma\sigma'}(i\omega_n,\boldsymbol{p}) \\ \hat{F}^{+}_{\sigma\sigma'}(i\omega_n,\boldsymbol{p}) & \hat{G}^{+}_{\sigma\sigma'}(i\omega_n,\boldsymbol{p}) \end{pmatrix}.$$

which in the momentum space is given by

$$\begin{aligned} \hat{G}_{\sigma\sigma'}(i\omega_n,\boldsymbol{p}) &= \delta_{\sigma\sigma'}\left(\frac{u_p^2}{i\omega_n-\varepsilon_p}+\frac{v_p^2}{i\omega_n+\varepsilon_p}\right), \\ \hat{F}_{\sigma\sigma'}(i\omega_n,\boldsymbol{p}) &= -i\sigma_y u_p v_p\left(\frac{1}{i\omega_n-\varepsilon_p}-\frac{1}{i\omega_n+\varepsilon_p}\right), \end{aligned}$$

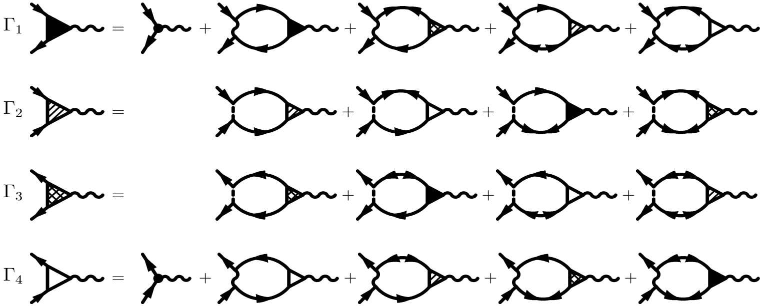

Figure: A diagrammatic representation of the coupled integral equations for the effective weak vertices in superfluid baryonic matter. The "normal" propagators for particles (holes) are shown by single-arrowed lines directed from left to right (right to left). The double arrowed lines correspond to the "anomalous" propagators $F$ (two incoming arrows) and $F^{+}$ (two outgoing arrows). The "normal" vertices $\Gamma_1$ and $\Gamma_4$ are shown by full and empty triangles. The "anomalous" vertices $\Gamma_2$ and $\Gamma_3$ are shown by hatched and shaded triangles. The horizontal wavy lines represent the low-energy propagator of $Z^0$ gauge boson. The vertical wavy lines stand for the particle-particle interaction $v_{pp}$, dashed lines - for particle-hole interaction $v_{ph}$.

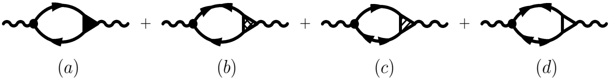


Figure: The sum of polarization tensors contributing to the vector-current neutrino emission rate. Note that the diagrams $b$, $c$, and $d$ are specific to the superfluid systems and vanish in the unpaired state.

The result can be cast as

$$\epsilon_V = \frac{G^2 c_V^2 N_f}{48\pi^4} \int_0^\infty d\omega g(\omega)\omega J(\omega),$$

where $c_V = 1$ for neutrons and $c_V = 0.08$ for protons, $N_f = 3$ is the number of neutrino flavors in the Standard Model, and

$$\begin{aligned} J_V(\omega) &= \int_0^\omega d\boldsymbol{q}\boldsymbol{q}^2(\boldsymbol{q}^2 - \omega^2)\mathrm{Im}\left[\Pi_{00}(\omega, q) - \Pi_{ii}(\omega, q)\right] \\ &= -\frac{8\omega^5 \nu(0) v_F^4}{405}\mathrm{Im}(F * F^+)_0[1 + \gamma v_F^2], \end{aligned}$$

# Vector current emissivity

The vector current emissivity is given by ($z = \Delta/T$)

$$\epsilon_V = \frac{16G^2 c_V^2 \nu(0) v_F^4}{1215\pi^3} J_V(z) T^7, \quad J_V(z) = z^7 \int_1^\infty \frac{dy\, y^5}{\sqrt{y^2-1}} f(zy)^2 \left[1 + \left(\frac{7}{33} + \frac{41}{77}\gamma\right) v_F^2\right].$$

Dependence of the integral on reduced temperature $T/T_c$ (Upper panel). Higher order corrections to the leading order result ('12)

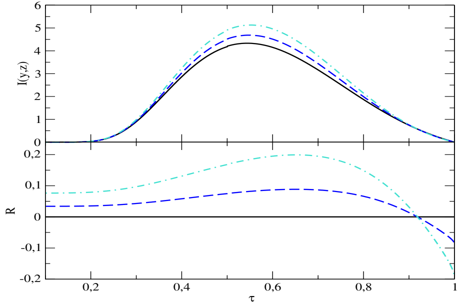

# Axial current emissivity

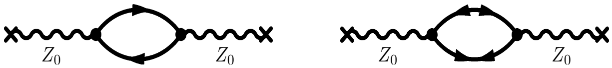


Figure: The two diagrams contributing to the polarization tensor of baryonic matter, which defines the axial vector emissivity. The "normal" baryon propagators for particles (holes) are shown by single-arrowed lines directed from left to right (right to left). The double arrowed lines correspond to the "anomalous" propagators $F$ (two incoming arrows) and $F^+$ (two outgoing arrows).

The emissivity of this processes is given by

$$\epsilon_A = \frac{4G_F^2 g_A^2}{15\pi^3}\zeta_A \nu(0) {v_F}^2 T^7 J_A, \quad J_A = z^7 \int_1^\infty dy \frac{y^5}{\sqrt{y^2-1}} f_F\,(zy)^2\,. \qquad (6)$$

Note the $v_F^2$ scaling of the axial neutrino emissivity compared to the $v_F^4$ scaling.

**Conclusion: Axial neutrino emissivity dominates the vector current emissivity because of $v^2$ scaling instead of $v^4$ scaling. (Opposite to the conclusion found in the classical paper by Flowers, Ruderman and Sutherland '76)**

# Axial current emissivity


Figure: The two diagrams contributing to the polarization tensor of baryonic matter, which defines the axial vector emissivity. The "normal" baryon propagators for particles (holes) are shown by single-arrowed lines directed from left to right (right to left). The double arrowed lines correspond to the "anomalous" propagators $F$ (two incoming arrows) and $F^+$ (two outgoing arrows).

The emissivity of this processes is given by

$$\epsilon_\nu = \frac{4G_F^2 g_A^2}{15\pi^3}\zeta_A \nu(0) {v_F}^2 T^7 I_\nu, \quad I_\nu = z^7 \int_1^\infty dy \frac{y^5}{\sqrt{y^2-1}} f_F\left(zy\right)^2 . \tag{7}$$

Note the $v_F^2$ scaling of the axial neutrino emissivity compared to the $v_F^4$ scaling.

**Conclusion: Axial neutrino emissivity dominates the vector current emissivity because of $v^2$ scaling instead of $v^4$ scaling.**

# Temperature evolution

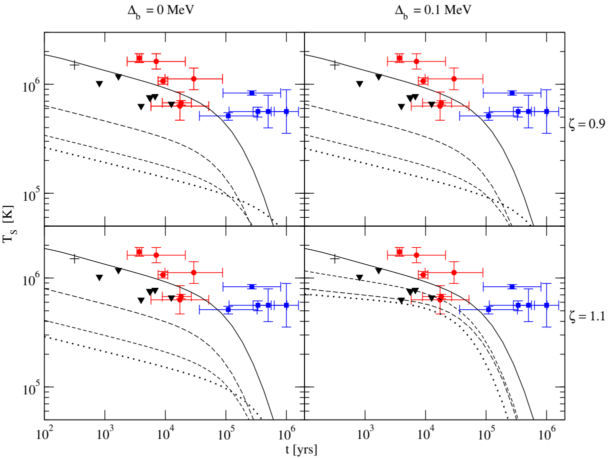


Cooling simulation of stars with quark matter cores, (D. Hess, A. Sedrakian, Phys. Rev. D 84, 063015 (2011))

# Temperature evolution

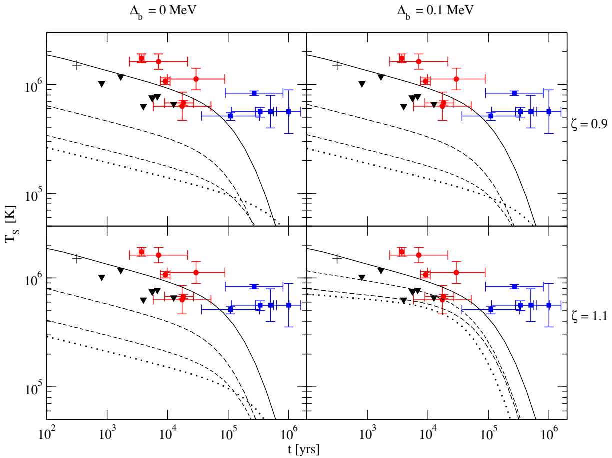


Cooling simulation of stars with quark matter cores, (D. Hess, A. Sedrakian, Phys. Rev. D 84, 063015 (2011))

# Compact star path on the phase diagram

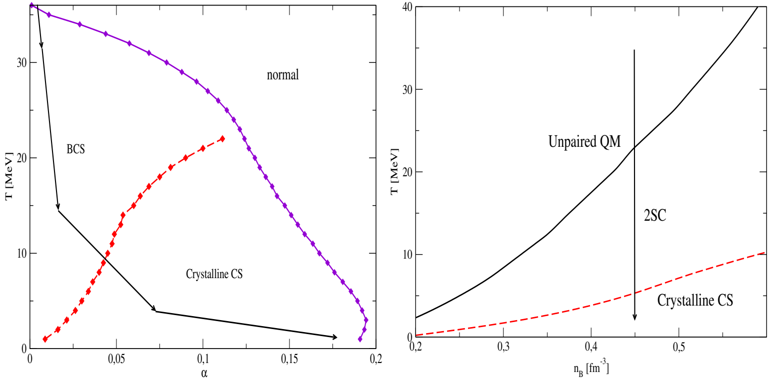


The path taken by a compact star in the phase diagrams.

# CAS A: a cooling quark star?

- Red-green quarks in the 2SC phase may or may not be fast cooling agents depending on the gaplessness parameter.
- The blue quarks act as a BCS superconductor and can contribute to fast cooling if their gaps are small, inversely, can be ineffective in cooling if their gaps are large.

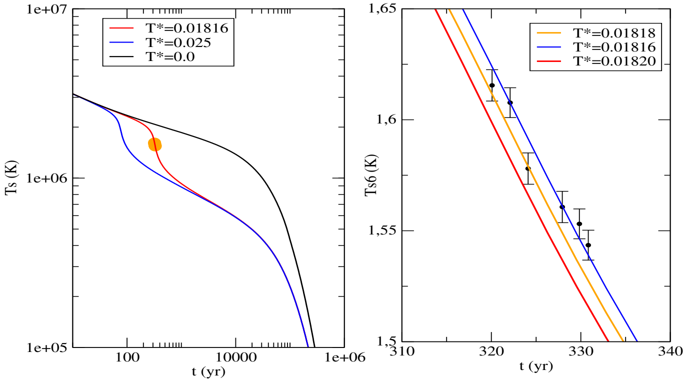

# Conclusions

- There is little doubt that
  there is enough room for massive compact stars to harbor some sort of exotic matter.
  In our models the central densities reach $10 \times \rho_0$.

- Mechanisms of accommodating exotic matter in compact stars require more repulsion in the quark and also in the hyper-nuclear sectors (reasonable so far!)

- Cooling simulations being sensitive to the composition of matter can be used to identify phase transitions to superfluid states (e.g. in color superconducting quark matter).